

Microstructure Analysis on Size Distribution During Film Growth in HAMR Media

Bing Zhou^{1,2}, B. S. D. C. S. Varaprasad^{1,3}, Enbo Zhang^{1,2}, David E. Laughlin^{1,2,3}, and Jian-Gang Zhu^{1,2,3}

¹Data Storage Systems Center, Carnegie Mellon University, Pittsburgh, PA 15213 USA

²Materials Science and Engineering Department, Carnegie Mellon University, Pittsburgh, PA 15213 USA

³Electrical and Computer Engineering Department, Carnegie Mellon University, Pittsburgh, PA 15213 USA

Grain size and size distribution reduction in L1₀ FePt granular thin film is becoming critical to increase the areal storage density and realize the full potential of heat-assisted magnetic recording media. FePt and amorphous carbon or mixture with other segregants are often deposited at elevated temperature in order to promote the L1₀ ordering in FePt. Due to the materials system and high temperature involved in the fabrication process, the bimodal distribution of the grains is often observed with a significant amount of small grains with diameter <3 nm. The bimodal distribution of the grains could potentially lead to a significant microstructure nonuniformity and thus grain-to-grain properties variation, such as Curie temperature (T_c), texture, ordering, and magnetic properties. In this paper, we performed a detailed analysis on microstructure evolution of FePt-C thin film during the growth process on different initial layer conditions to understand the origin of bimodal grain size distribution in the FePt-C media. Experimental modeling study of depositing FePt on continuous carbon layer at elevated temperature was conducted to understand the nucleation and growth process.

Index Terms—Bimodal distribution, grain size distribution, L1₀ FePt, nucleation and growth.

I. INTRODUCTION

GRANULAR L1₀-ordered FePt is well known to be the most promising candidate for a heat-assisted magnetic recording (HAMR) media material due to its high magnetocrystalline anisotropy [1], [2]. Amorphous carbon is often used as a part of the grain boundary materials to obtain well-isolated FePt grains with small grain size due to their strong phase separation tendency. High temperature has to be used during the deposition process to promote L1₀ ordering in FePt. Although the high magnetocrystalline anisotropy of FePt L1₀ phase allows very small thermally stable grains in principle, it is very challenging to achieve the microstructure with grains of such small mean grain diameter and narrow grain size distribution in reality due to the material system and the fabrication process. In particular, it has been reported in many literature that bimodal distribution of FePt grain size is present in FePt(Ag)-X thin film with X = C or mixture of C with other oxides and nitrides [3]–[6]. It is observed that the fraction of small grains with diameter <3 nm generally increases with the increasing volume fraction of C in the thin film. By replacing a part of C with boron nitride and utilizing laminated multilayer growth method, the fraction of small grains can be controlled to some extent [7]. Due to the lateral growth of the FePt grains during film deposition process at elevated temperature, these small grains often located in between several large grains could potentially serve as the merging point between the neighboring grains. The presence of the bimodal distribution in the FePt-C-based media will become a more important consideration when the mean grain

size and pitch distance are further pushed down to increase the areal density of HAMR media, since it will lead to nonuniformity in grain size, ordering, texture, magnetic properties, and eventually contribute to transition jitter noise and significant reduction in the media signal-to-noise ratio [8]–[11].

It was proposed that the formation of the small grains could be governed by inherent properties of the segregant to FePt interface [7]. In this paper, we performed detailed analysis on microstructure evolution of the FePt-C media with different grain size distribution profiles in the early stage of the film growth to show that the nucleation of FePt grains on MgO surface can be a continuous process throughout the film deposition. At elevated temperature, FePt atoms can penetrate through carbon and nucleate on MgO surface due to high surface mobility of carbon. Therefore, new FePt grains can nucleate at all stages of the film growth until the packing fraction becomes high while the prenucleated grains keep on growing laterally (increase in diameter). The difference in growth rate of the small and large grains at the later stage of film growth leads to bimodal distribution. This continuous nucleation process of FePt grains throughout film growth is one of the fundamental reasons behind the broad size distribution in the FePt-C media.

II. EXPERIMENTAL SETUP

All films were sputtered on thermally grown a-SiO₂ substrates using an AJA Orion-8 system with base pressure better than 5×10^9 Torr. All substrates are cleaned by acetone, isopropyl alcohol, deionized water, and dry etching by O₂ plasma. For all samples, MgO was RF sputtered at 10 mTorr at room temperature. In sample series A, the film stack is Si|SiO₂|MgO (9 nm)|FePt + 34 vol.%C (*t* nm), where *t* = 1.5 and 7 nm for A1 and A2, respectively. The deposition pressure was at

Manuscript received March 16, 2018; accepted April 18, 2018. Corresponding author: B. Zhou (e-mail: bingzhou@andrew.cmu.edu).

Color versions of one or more of the figures in this paper are available online at <http://ieeexplore.ieee.org>.

Digital Object Identifier 10.1109/TMAG.2018.2829921

TABLE I
SPUTTERING PRESSURES AND RATES OF ALL MATERIALS

Materials	Pressure (mTorr)	Deposition rate (nm/min)
MgO	10	0.55
FePt	5	1.08
	20	0.30
C	5	0.56
	20	0.15

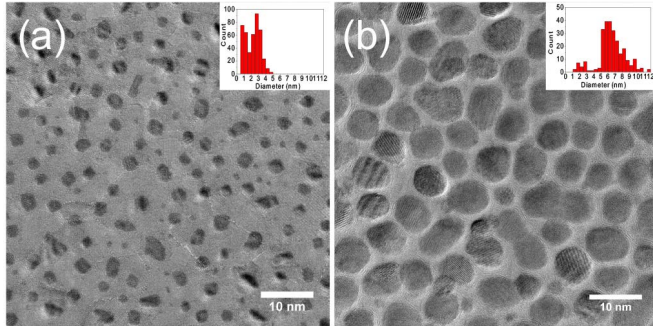


Fig. 1. In-plane HR-TEM image of the film stack Si|SiO₂|MgO (9 nm)|FePt + 34 vol.%C (t nm) with (a) $t = 1.5$ nm (A1) and (b) 7 nm (A2).

5 mTorr for both samples. In sample series B, the film stack was same as series A with $t = 1.5, 3, 4, 6,$ and 7 nm for samples B1–B5. The deposition pressure of B1 was kept at 20 mTorr to modify the microstructure of FePt grains in the initial stage of film growth. For samples B2–B5, the deposition pressure was kept at 20 mTorr for the first 1.5 nm FePt-C and 5 mTorr for the rest of the film thickness. In sample series A and B, FePt and C were cosputtered onto the predeposited MgO layer at 650 °C to promote L1₀ ordering. In order to show the diffusion of FePt atoms through carbon and nucleate on MgO surface, a modeling experiment was conducted on sample C with the film stack being Si|SiO₂|MgO (9 nm)|C (4 nm)|FePt (1.5 nm). The continuous carbon layer was deposited at room temperature at 5 mTorr and subsequently the FePt layer was deposited at 650 °C at 5 mTorr onto the carbon layer. The sputtering pressure and rates of all materials are summarized in Table I. The cross section transmission electron microscope (TEM) image was examined to identify the location where FePt grains nucleate. The in-plane and cross section microstructure of all samples were examined using TEM. Multiple numbers of plane view high-resolution TEM (HR-TEM) images, taken from different regions of each sample, are used for calculating the statistical grain size distribution histogram with the total number of grains counted exceeding 500.

III. RESULT AND DISCUSSION

A. Bimodal Distribution Starts From Initial Stage of Film Growth

Fig. 1(a) and (b) shows the microstructure of initial stage (A1) and the final stage (A2) of the FePt-C media deposited at low pressure (5 mTorr). It can be clearly seen that the bimodal distribution of FePt grains starts from the initial stage of the film growth. In the initial stage shown in Fig. 1(a), the major peak is around 2.5–3 nm, while the

minor peak is around 1 nm. Both peaks shift toward right in the final stage of film growth with the major peak shifts from 6 to 7 nm, while the minor peak shifts to around 2 nm. At low deposition pressure, the incident angle distribution of FePt atoms is narrow and the mean free path of FePt atoms is long due to less collision with Ar atoms when they travel from the target to the MgO underlayer. As a result, the ad-atoms tend to have high surface mobility due to high kinetic energy when they arrive upon the surface of the MgO underlayer. Due to the high surface mobility of FePt atoms and narrow incident angle distribution, the probability of newly sputtered FePt atoms colliding with each other forming new nucleus in between the preexisting FePt nuclei is high. Therefore, the bimodal distribution of grain size is observed in the initial stage. In this case, the bimodal distribution of grain size observed in the final stage of the film growth can be caused by the following two possible reasons: 1) all grains nucleate in the initial stage of the film growth, but some grains preferentially grow faster than others during the film growth process and 2) the small FePt grains could be nucleated on the MgO surface throughout the film growth process, as long as the space between the preexisting grains is large enough. In order to study the effect of the initial size distribution on the final size distribution, sample series B with optimized grain size distribution in initial stage was conducted.

B. Microstructure Evolution of FePt-C Media With Optimized Initial Stage of Film Growth

By tuning the deposition pressure from 5 to 20 mTorr, the size distribution of FePt grains can be modified to single peak distribution in the initial stage of 1.5 nm FePt-C, shown in Fig. 2(a). As the film thickness increases to 3 nm, single peak shape is retained in grain size distribution histogram, though the grain size distribution becomes wider and the peak shifts to around 4 nm, shown in Fig. 2(b). The bimodal distribution in grain size is first observed at the film thickness of 4 nm, shown in Fig. 2(c). The small grains (<3 nm) and the large grains (>7.5 nm) account for 20% and 2% of the total number of grains at this stage, respectively. As the film thickness continues to increase to 6 and 7 nm, the fraction of the large grains increases to 9% and 16%, respectively, while the fraction of the small grains decreases to 15% and 9%, respectively, of the total number of grains. From the cross section TEM images shown in Fig. 2(f) and (g), the small grains (marked by red circles) are sitting on the MgO surface and the distribution of grain height is observed. The second layer of FePt grains (marked by blue circles) started to form when the film thickness increases to 7 nm. This shows that the small grains we observed in samples with film thickness <6 nm are not the second layer of FePt grains sitting on carbon, but FePt grains nucleating on the surface of MgO.

Regardless of the grain size distribution profile in the initial stage, shown in Figs. 1(a) and 2(a), the bimodal distribution of grains will appear in the final stage of the film growth, shown in Figs. 1(b) and 2(e). Fig. 3 shows the HR-TEM images from sample B3 and the small grains <3 nm are circled using dotted lines. It is interesting that the small grains

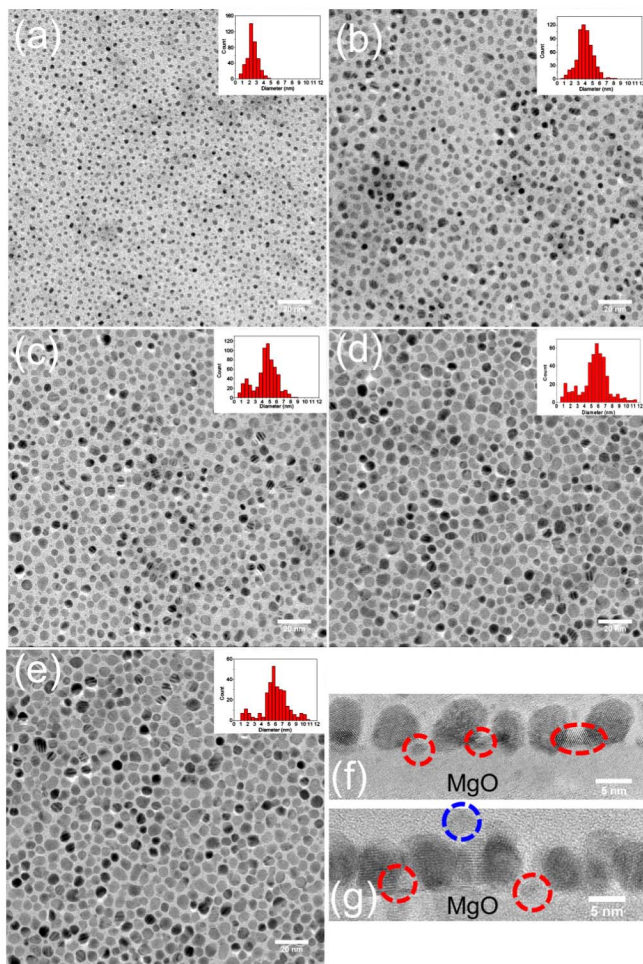


Fig. 2. In-plane bright-field TEM images of the film stack Si|SiO₂|MgO (9 nm)|FePt + 34 vol.%C (t nm) with (a) $t = 1.5$ nm (B1), (b) 3 nm (B2), (c) 4 nm (B3), (d) 6 nm (B4), and (e) 7 nm (B5). High-resolution cross section TEM images of (f) samples B4 and (g) B5. Red dotted circles: small grains nucleated on MgO surface. Blue dotted circles: second layer of grains nucleated on carbon.

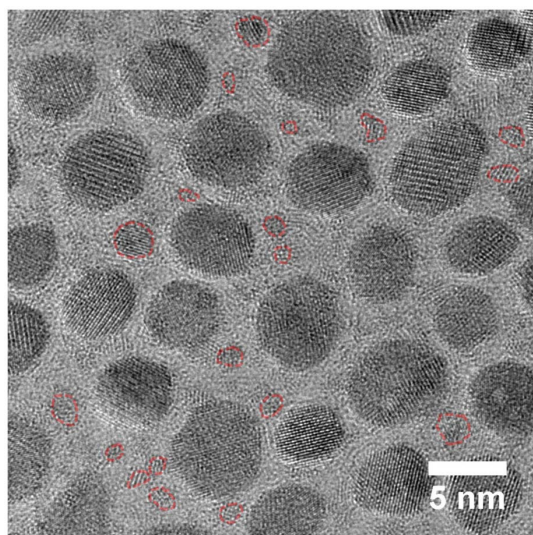


Fig. 3. In-plane HR-TEM image of sample B3. Dotted circle: small grains with diameter < 3 nm.

are often located in the middle region between several large grains, which is covered by amorphous carbon. This infers that FePt atoms could possibly penetrate through amorphous

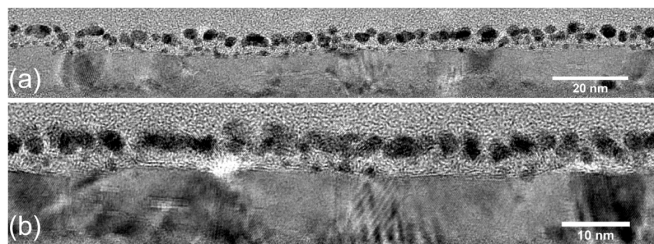


Fig. 4. (a) Bright field and (b) high resolution cross section TEM images of sample C with the film stack Si|SiO₂|MgO (9 nm)|C(4 nm)|FePt (1.5 nm).

carbon and form a stable nucleus in the region, where the available space is large. This could be the potential reason causing the microstructure consisting of small grains sitting in between several large grains as shown in Fig. 3.

C. Model Experiment: FePt Penetrate Through Continuous Carbon Thin Film

In order to verify the hypothesis that FePt atoms can penetrate through carbon and forming stable nuclei on MgO surface due to high surface mobility of carbon at elevated temperature, the sample C with film stack of Si|SiO₂|MgO (9 nm)|C (4 nm)|FePt (1.5 nm) was fabricated. As shown in Fig. 4(a) and (b), the cross section TEM image, there are clearly two types of FePt grains formed. The FePt grains nucleated on top of the continuous carbon layer with size around 3 ~ 5 nm and FePt grains nucleating on the MgO surface with size around 1 ~ 2 nm. It shows that the FePt ad-atoms could potentially penetrate through carbon and form stable nuclei on MgO surface, even though the carbon layer is continuous. As the small nuclei are immersed in a relatively C-rich environment, the FePt ad-atoms arriving on the film at a later stage will have comparably limited probability to attach to them compared with the ones nucleating on top of the carbon layer. Therefore, the growth rate of the small grains is much lower compared with the ones nucleating on top of carbon, even if both of them start with similar size of nuclei. The analogy can be taken to the film growth process as shown in Fig. 2. Although the grain size distribution shows a single peak for the film below 3 nm, the deposited FePt atoms can penetrate through carbon at elevated deposition temperature due to the high surface mobility of carbon and form stable nuclei in between the large grains, where the available space is large. This continuous nucleation of new FePt grains dominates in the initial and the middle stages of the film growth process when the packing fraction is relatively low, but it becomes slower and eventually stops as the packing fraction increases. Due to the C-rich environment surrounding the small nuclei, their accessibility to the newly deposited FePt atoms is limited compared with the larger grains. Additionally, the height distribution of FePt grains induces a shadowing effect during film growth, which further slows down the growth rate of small FePt grains. This limited growth of small FePt grains becomes more dominant at later stage of film growth, when C surrounding small FePt grains becomes richer and the shadowing effect becomes more significant

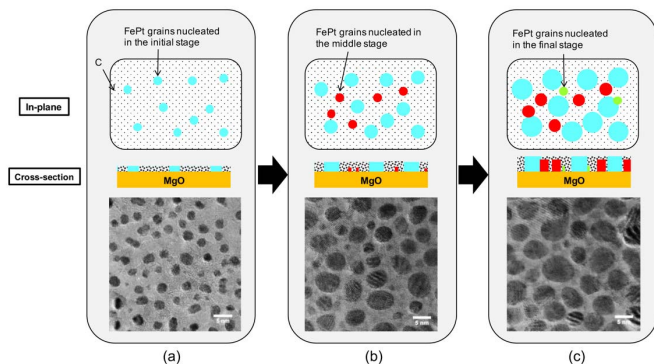


Fig. 5. In-plane and cross section schematic drawing present the microstructure evolution of (a) initial stage, (b) middle stage, and (c) final stage during film growth with the in-plane HR-TEM images of each stage.

due to height variation between grains. As the film thickness increases, FePt grains grow laterally and eventually merge with the neighboring FePt grains. Therefore, at the later stage of the film growth, the fraction of small grains (<3 nm) decreases, while the fraction of the large grains (>7.5 nm) increases. The film growth process is illustrated in the schematics shown in Fig. 5. Note that the schematic is not drawn on scale and the actual FePt grain shape may be different.

IV. CONCLUSION

We have conducted a systematic study on the grain size distribution in FePt-C granular HAMR media on MgO underlayer. It is found that the nucleation of new FePt grains can happen at any stage of the film growth on MgO surface until the packing fraction becomes high. Carbon grain boundary does not seem to prevent such continuous nucleation of new grains throughout the film growth. As the film grows thicker, most of the FePt grains nucleated earlier grow laterally at a similar rate while the new grains keep on forming. Consequently, it leads to either bimodal grains size distribution or broader grain size distribution in the later stage of the film growth. It is also found that even though the grain

size distribution can be controlled to be relatively more uniform in the initial stage, it does not prevent the lateral growth of the existing grains and formation of new grains which happens concurrently at the later stage of the film growth.

ACKNOWLEDGMENT

This work was supported in part by Western Digital, Seagate Technology, in part the Data Storage Systems Center, Carnegie Mellon University, and in part by the Materials Characterization Facility, Carnegie Mellon University under Grant MCF-677785.

REFERENCES

- [1] M. H. Kryder *et al.*, "Heat assisted magnetic recording," *Proc. IEEE*, vol. 96, no. 11, pp. 1810–1835, Nov. 2008.
- [2] A. Perumal, Y. K. Takahashi, and K. Hono, " L_{10} FePt-C nanogranular perpendicular anisotropy films with narrow size distribution," *Appl. Phys. Express*, vol. 1, no. 10, p. 101301, 2008.
- [3] D. Weller, O. Mosendz, G. Parker, S. Pisana, and T. S. Santos, " L_{10} FePtX-Y media for heat-assisted magnetic recording," *Phys. Status Solidi A Appl. Mater. Sci.*, vol. 210, no. 7, pp. 1245–1260, 2013.
- [4] O. Mosendz, S. Pisana, J. W. Reiner, B. Stipe, and D. Weller, "Ultra-high coercivity small-grain FePt media for thermally assisted recording (invited)," *J. Appl. Phys.*, vol. 111, no. 7, p. 07B729, 2012.
- [5] B. S. D. C. S. Varaprasad, M. Chen, Y. K. Takahashi, and K. Hono, " L_{10} -ordered FePt-based perpendicular magnetic recording media for heat-assisted magnetic recording," *IEEE Trans. Magn.*, vol. 49, no. 2, pp. 718–722, Feb. 2013.
- [6] K. Hono and Y. K. Takahashi, " L_{10} -FePt granular films for heat-assisted magnetic recording media," in *Ultra-High-Density Magnetic Recording Storage Materials and Media Designs*, G. Varvaro and F. Casoli, Eds. Singapore: Pan Stanford, 2016, ch. 5, pp. 245–277.
- [7] D. Weller *et al.*, "Review Article: FePt heat assisted magnetic recording media," *J. Vac. Sci. Technol. B, Nanotechnol. Microelectron., Mater. Process., Meas., Phenomena*, vol. 34, no. 6, p. 060801, 2016.
- [8] J. G. Zhu and H. Li, "Signal-to-noise ratio impact of grain-to-grain heating variation in heat assisted magnetic recording," *J. Appl. Phys.*, vol. 115, no. 17, p. 17B747, 2014.
- [9] H. Li and J.-G. Zhu, "The role of media property distribution in HAMR SNR," *IEEE Trans. Magn.*, vol. 49, no. 7, pp. 3568–3571, Jul. 2013.
- [10] S. Pisana *et al.*, "Curie temperature distribution in FePt granular media," *IEEE Trans. Magn.*, vol. 51, no. 4, Apr. 2015, Art. no. 3200205.
- [11] A. Chernyshov *et al.*, "Measurement of magnetic properties relevant to heat-assisted-magnetic-recording," *IEEE Trans. Magn.*, vol. 49, no. 7, pp. 3572–3575, Jul. 2013.